JOURNAL OF MAGNETIC RESONANCE **125,** 220–223 (1997)
ARTICLE NO. MN961102

Dipolar Oscillations in Cross-Polarized Peptide Samples in Oriented Lipid Bilayers

F. TIAN AND T. A. CROSS

Center for Interdisciplinary Magnetic Resonance at the National High Magnetic Field Laboratory, Institute of Molecular Biophysics, and Department of Chemistry, Florida State University, Tallahassee, Florida 32306

Received December 17, 1996

Two of the fundamental challenges in biological solid-state NMR are the needs for sensitivity and resolution. Here we scrutinize the cross-polarization conditions for a hydrated and uniformly aligned lipid bilayer preparation of a polypeptide. Mixing times on the millisecond time scale used in cross-polarization lead to uniform spin temperature and relatively uniform sensitivity enhancements for a variety of chemical sites. However, long mixing times result in less than maximal sensitivity for some sites and the loss of selectivity which can lead to a loss of spectral resolution. Dipolar oscillations as a function of mixing time are observed in the samples studied here. These oscillations lead to improvements in sensitivity and spectral resolution as well as a measure of the dipolar interaction magnitude, the ^{1}H spin diffusion rates, and an upper limit on hydrogen exchange rates. The field-dependent $T^{\mathrm{H}}_{1\rho}$ relaxation rates are also measured.

Ernst and co-workers (*1*) observed transient oscillations in protonated ^{13}C spectra of ferrocene with short mixing times. The oscillation frequency was shown to represent the orientation-dependent dipolar interaction between the observed rare nuclei and the directly bonded protons. Because of the r^{-3} distance dependence, the directly attached proton dominates the calculation of the dipolar interaction. Depolarization and polarization-inversion pulse sequences have taken advantage of such oscillations to enhance the selection of certain spin populations (*2–4*). These dipolar oscillations have also been reported in several other studies (*5, 6*).

Recently, we have shown that complete three-dimensional structures can be obtained from orientational constraints derived from solid-state NMR (*7, 8*). These structural constraints derive from samples that are uniformly aligned with respect to the magnetic field, such that the orientation-dependent frequencies of various nuclear spin interactions can be observed (*9–12*). Most of these constraints have been obtained from polypeptides isotopically labeled at a single site, but current research is focused on obtaining such constraints from amino-acid-specific labeling and from uniform isotopic labeling (*13*). For such multidimensional experiments, sensitivity and resolution are a primary concern. Consequently, there is great interest in taking these experiments to high field. When spectral linewidths cannot be further

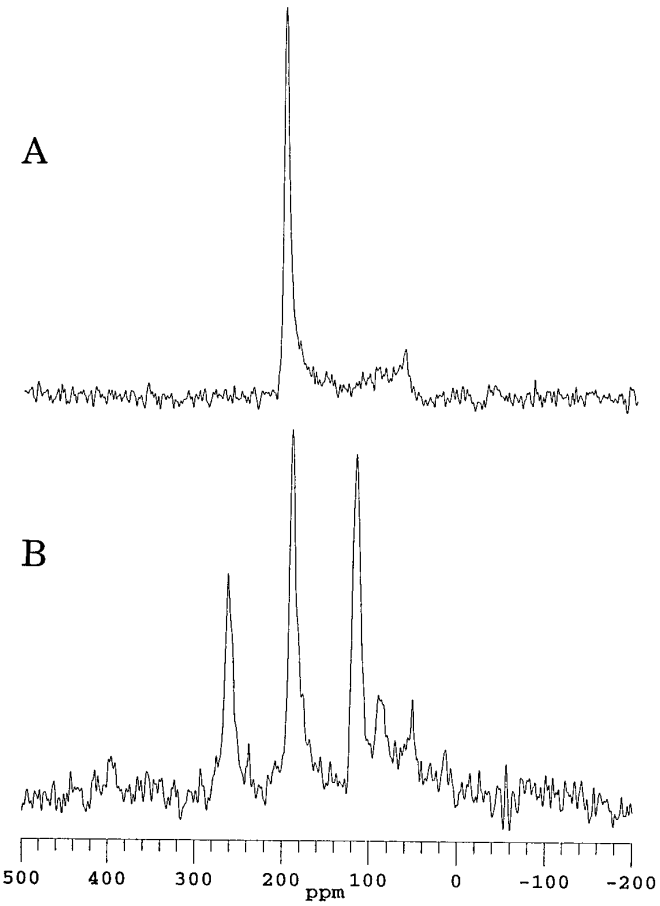

FIG. 1. ^{15}N spectra at 40 MHz of 30 mg $^{15}N_{1,3,5,7}$ gramicidin A in hydrated (50% by weight) DMPC lipid bilayer (1:8 molar ratio) oriented with the bilayer normal parallel to the magnetic field direction. The cross-polarized spectra were obtained with spectral width 60 kHz and acquisition time 8.55 ms. (A) 50 μs contact time, 3.0 s recycle delay, and 600 acquisitions; (B) is from the same sample after exposure to a D_2O atmosphere for 2 days obtained with a 1.2 ms contact time and 2400 acquisitions.

1090-7807/97 $25.00

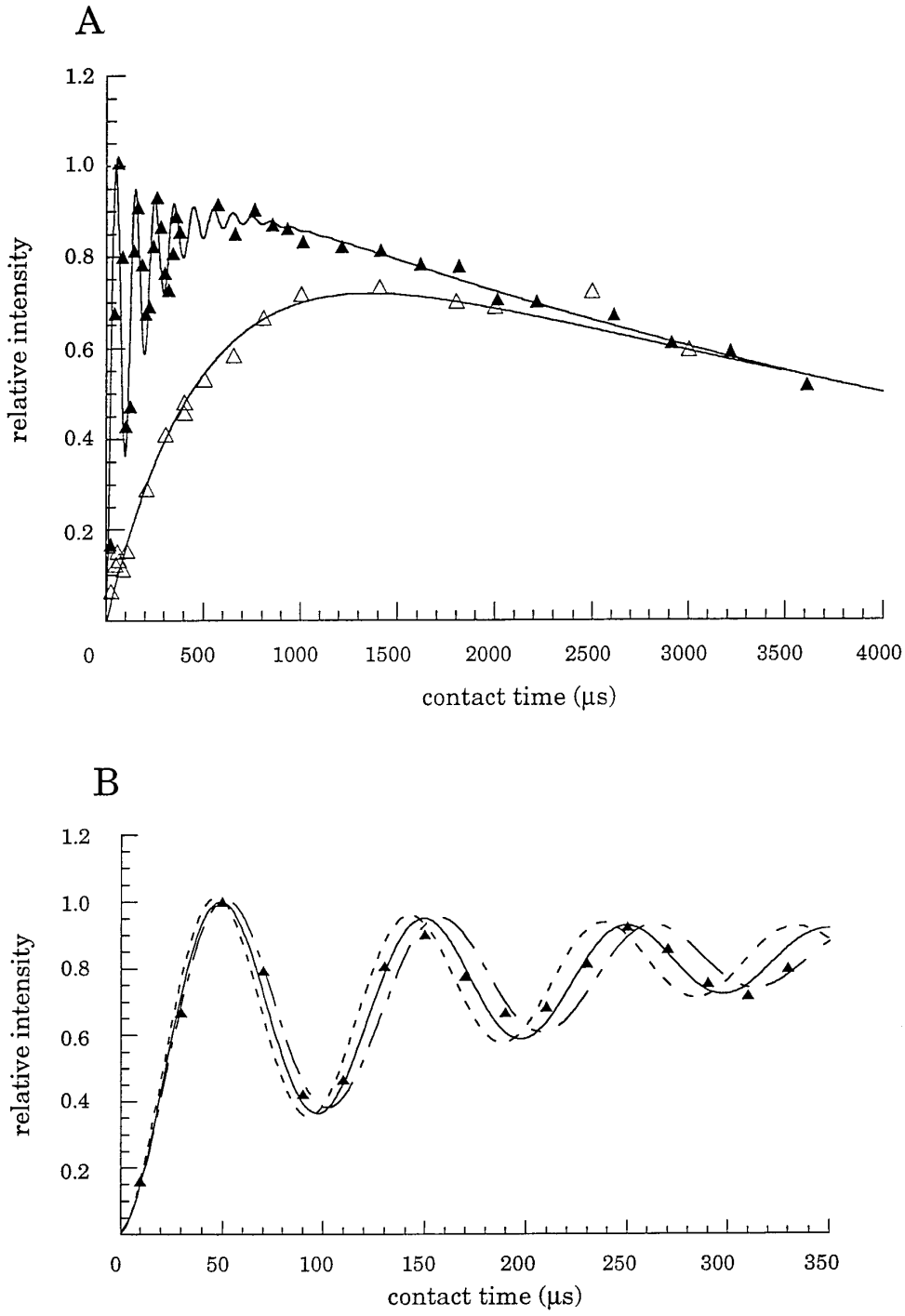

FIG. 2. ^{15}N signal intensity versus contact time. (A) ▲ corresponds to experimental data for the protonated sites and the solid line is the simulation using Eq. [1] with a spin-diffusion rate $R^{-1} = 280\ \mu s$; $T_{1\rho}^{H} = 5.4$ ms, and the N–H dipolar interaction $\Delta\nu = 20$ kHz; △ corresponds to experimental data from the deuterated sample and, the solid line is the simulation using Eq. [2] with $T_{1\rho}^{H} = 5.4$ ms, $T_{NH} = 500\ \mu s$, and $T_{NH}/T_{1\rho}^{N} \cong 0$. (B) Expansion of the early part of (A) with the following simulations added: (---) $\Delta\nu = 21$ kHz, (-–-) $\Delta\nu = 19$ kHz.

reduced, spectral resolution can still be improved by selecting a subset of resonances. Through the use of short mixing times, it is possible to select for such resonance subsets.

Figure 1 shows spectra of $^{15}N_{1,3,5,7}$-labeled gramicidin A in a hydrated lipid bilayer. In such oriented samples, each of these sites contributes to a signal at 198 ppm. Figure 1A shows the high sensitivity of this sample in an Oxford Instruments widebore 9.4 T magnet observed with a home-

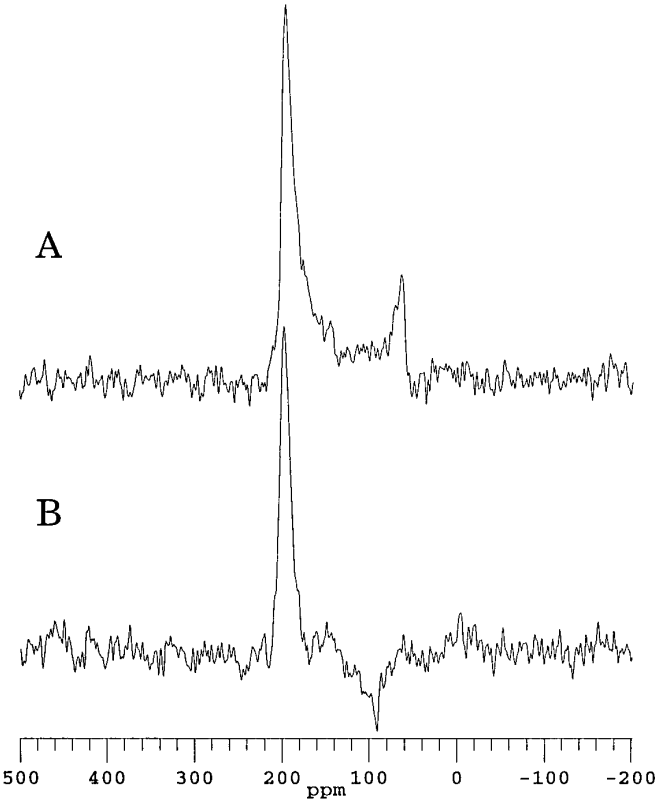

FIG. 3. ^{15}N spectra of $^{15}N_{1,3,5,7}$ gramicidin A using (A) a standard cross-polarization pulse sequence with 1 ms cross-polarization time and (B) a selective-polarization pulse sequence (*3*) with cross-polarization time 1 ms and polarization inversion time 50 μs.

built probe and homebuilt triple-resonance spectrometer assembled around a Chemagnetics data-acquisition system. This spectrum has been obtained with a 50 μs mixing time that provides a 10–15% improvement in sensitivity over a 1 ms mixing time (Fig. 2). Residual powder pattern intensity is observed primarily at the $\sigma_\perp$ edge of the spectrum (65 ppm). Figure 1B is a spectrum of the same sample after it was exposed to a D_2O atmosphere for two days. The nominal 1:1:1 triplet arises from the dipolar coupling between a spin-$\frac{1}{2}$ ^{15}N site and the directly attached spin-1 ^2H site. Note that the powder pattern intensity also shows the results of this dipolar coupling. The spectrum was obtained with a mixing time of 1.2 ms and would have shown very poor sensitivity if recorded at 50 μs (see Fig. 2).

Figure 2 shows the dipolar oscillations that occur as a function of mixing time. Simulations have been generated by modeling the magnetization, M, as a function of $T_{1\rho}^{H}$, the spin diffusion rate, R, and $\Delta\nu$, the magnitude of the dipolar interaction using the following equation modified from Müller *et al.* (*1*):

$$M_{(t)} = M_{(0)}e^{-t/T_{1\rho}^{H}}\left(1 - 0.5e^{-Rt} - 0.5e^{-1.5Rt}\cos\frac{\Delta\gamma t}{2}\right). \quad [1]$$

From separated-local-field experiments, the dipolar interaction for these four ^{15}N-labeled sites varies from 19.7 to 22 kHz (*7*). The observed dipolar oscillation frequency is just half of the dipolar splitting. Figure 2B shows simulations of the oscillation with a dipolar interaction of 20 $\pm$ 1 kHz. The dipolar oscillations damp away with the spin-diffusion rate, which is modeled here as R^{-1} = 280 μs. The remaining magnetization decay constant ($T_{1\rho}^{H}$) is assessed by observing the magnetization at long mixing times (Fig. 2A). For this data obtained at 9.4 T, $T_{1\rho}^{H}$ = 5.4 ms.

Figure 2A also shows the magnetization built up for a deuterated sample. Here no N–H dipolar oscillations are observed and the buildup is much slower, since multiple ^1Hs are involved and the ^1Hs are further away from the ^{15}N site. Using the following expression (*14*) with the same value of $T_{1\rho}^{H}$, T_{NH} = 500 μs, and $T_{NH}/T_{1\rho}^{N} \approx 0$, the $^{15}N-{}^2H$ data were simulated,

$$M_{(t)} = M_{(0)}e^{-t/T_{1\rho}^{H}}\lambda^{-1}(1 - e^{-\lambda t/T_{NH}}), \quad [2]$$

where

$$\lambda = \left(1 + \frac{T_{NH}}{T_{1\rho}^{N}} - \frac{T_{NH}}{T_{1\rho}^{H}}\right).$$

Equations [1] and [2] both reduce to

$$M_{(t)} = M_{(0)}e^{-t/T_{1\rho}^{H}} \quad [3]$$

at long mixing times. If $^{15}N-{}^1H$ and $^{15}N-{}^2H$ sites were both present in a sample, a factor of 7 enhancement of

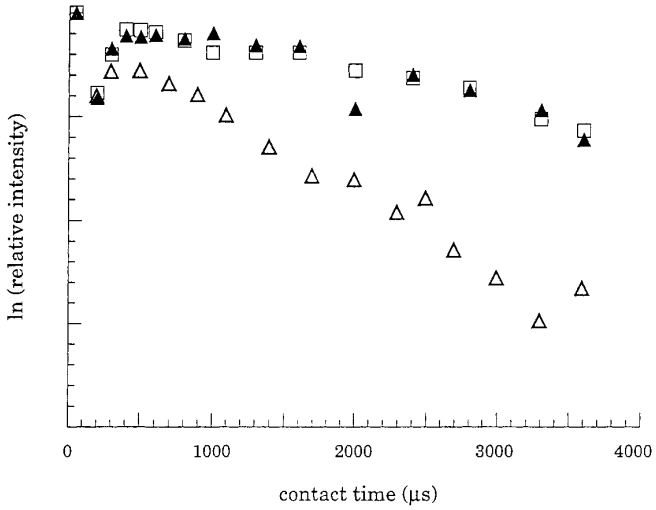

FIG. 4. Dependence of $T_{1\rho}^{H}$ on B_0 and B_1. (▲) and (□) represent the experimental data from a 9.4 T field with B_1 = 38 kHz and B_1 = 56 kHz, respectively, $T_{1\rho}^{H}$ = 5.4 ms; Δ is from a 4.7 T field with B_1 = 37 kHz and $T_{1\rho}^{H}$ = 2.2 ms.

the protonated sites could be achieved relative to the deuterated sites by using a short mixing time (e.g., 50 μs for the data shown in Fig. 2A). Moreover, as shown in Fig. 3 by using a polarization-inversion sequence (*2*), specific regions of the spectrum can be enhanced. Here portions of the sample that are well aligned between glass plates are enhanced over those portions of the sample that have been squeezed out from between the glass plates and now result in unoriented powder pattern intensity.

In Fig. 4, relatively long mixing times are used to illustrate the $T_{1\rho}^{H}$ dependence on B_1 and B_0 fields. The increase in relaxation time with increasing B_0 suggests the potential for narrower resonances in the PISEMA experiment (*15*) where the linewidths are limited by $T_{1\rho}^{H}$ in high field. Therefore, higher fields will not only result in improved chemical-shift dispersion, but there is also a possible improvement in linewidth, not on just the ppm scale, but on the hertz scale. Again higher fields will result in higher sensitivity, not only through the Boltzmann factor and possible improvements in the linewidth, but potentially through the use of multiple-contact cross polarization, a technique applied rather infrequently in solids because few samples have long $T_{1\rho}^{H}$. Furthermore, these contacts can be made very short to obtain optimal sensitivity in these aligned samples.

The observed dipolar oscillations have a variety of potential applications. Not only can the oscillation frequency be used to enhance and improve the resolution, but it can be directly interpreted as a dipolar magnitude and hence dipolar vector orientation in aligned samples. The very efficient transfer of magnetization also has potential applications in experiments such as heteronuclear correlation solid-state NMR spectroscopy (*16*). In addition, the observed spin-diffusion rate places an upper limit on the proton exchange rate of 280 μs, consistent with a variety of additional data on the backbone amide exchange rates (*17*).

ACKNOWLEDGMENTS

The authors are indebted to A. Blue of the staff of the NHMFL CIMAR Program; to J. Vaughn, R. Rosanske, and T. Gedris of the staff of the FSU NMR Facility for their skillful maintenance and service of the NMR spectrometers; and to H. Henricks and U. Goli in the Bioanalytical Synthesis and Services Facility for their expertise and maintenance of the ABI 430A peptide synthesizer and HPLC equipment. This work has been supported by NSF Grant DMB 9317111.

REFERENCES

1. L. Müller, A. Kumar, T. Baumann, and R. R. Ernst, *Phys. Rev. Lett.* **32,** 1402 (1974).
2. X. L. Wu, S. M. Zhang, and X. W. Wu, *J. Magn. Reson.* **77,** 343 (1988).
3. X. L. Wu and S. M. Zhang, *Chem. Phys. Lett.* **156,** 79 (1989).
4. X. L. Wu and K. W. Zilm, *J. Magn. Reson. A* **104,** 119 (1993).
5. G. E. Hawkes, M. D. Mantle, K. D. Sales, S. Aime, R. Goberto, and C. J. Groombridge, *J. Magn. Reson. A* **116,** 251 (1995).
6. R. Pratima and K. V. Ramanathan, *J. Magn. Reson. A* **118,** 7 (1996).
7. R. R. Ketchem, W. Hu, and T. A. Cross, *Science* **261,** 1457 (1993).
8. R. R. Ketchem, B. Roux, and T. A. Cross, *in* ''Membrane Structure and Dynamics'' (K. M. Merz and B. Roux, Eds.), Birkhauser, Boston, 1996.
9. T. A. Cross and S. J. Opella, *Curr. Opin. Struct. Biol.* **4,** 574 (1994).
10. T. A. Cross, *Annu. Rep. NMR Spectrosc.* **29,** 123 (1994).
11. T. A. Cross, *in* ''Encyclopedia of NMR'' (D. M. Grant and R. K. Harris, Eds.), p. 2234, Wiley, New York, 1996.
12. S. J. Opella and D. A. McDonnell, *in* ''NMR in Proteins'' (G. M. Clore and A. M. Gronenborn, Eds.), CRC Press, Boca Raton, Florida, 1993.
13. R. Jelinek, A. Ramamoorthy, and S. J. Opella, *J. Am. Chem. Soc.* **117,** 12,348 (1995).
14. D. E. Axelson, ''Solid State Nuclear Magnetic Resonance of Fossil Fuels,'' Multiscience, Canada, 1985.
15. C. H. Wu, A. Ramamoorthy, and S. J. Opella, *J. Magn. Reson. A* **109,** 270 (1994).
16. P. Caravatti, L. Braunschweiler, and R. R. Ernst, *Chem. Phys. Lett.* **100,** 305 (1982).
17. S. Huo, S. Arumugam, and T. A. Cross, *Solid State NMR* **7,** 177 (1996).